2016 American Control Conference (ACC)
Boston Marriott Copley Place
July 6-8, 2016. Boston, MA, USA

An Experimental Evaluation of the Forward Propagating Riccati Equation to Nonlinear Control of the Quanser 3 DOF Hover Testbed

Anna Prach[1], Erdal Kayacan[1] and Dennis S. Bernstein[2]

***Abstract*— This study presents an experimental evaluation of the forward-propagating Riccati equation (FPRE) control. FPRE employs a state-dependent coefficient (SDC) parameterization of the nonlinear dynamics, and the feedback gains are updated in real time. The efficacy of the proposed control algorithm is verified by experimental studies on the Quanser 3 DOF Hover system. The ability of FPRE to follow the desired references is investigated, and its performance is compared with the conventional linear-quadratic regulator. Experimental results show the effectiveness of FPRE for following given references in the considered operating envelope.**

I. INTRODUCTION

In the absence of model uncertainty, nonlinearity, and computational constraints, it can reasonably be argued that linear-quadratic regulator (LQR) and linear-quadratic-Gaussian (LQG) control laws definitively solve the feedback control problem. In particular, assuming a full-order dynamic compensator, LQG can be used for stabilization, command following, and disturbance rejection for multiple-input, multiple-output (MIMO) plants with arbitrary channel coupling, arbitrary order and relative degree, and arbitrary poles and zeros.

In contrast to the case of linear plants, feedback control of nonlinear systems presents diverse challenges. A plant may have input and output nonlinearities (such as saturation and deadzone) due to sensor and actuator nonlinearities, and it may have nonlinearities that give rise to dynamics (such as limit cycles) that have no counterpart in the case of linear systems. In addition, there exist nonlinear systems (such as the nonholonomic integrator) that cannot be stabilized by any linear controller.

In view of the challenges mentioned above, it is not surprising that a vast range of techniques have been developed for nonlinear systems. These include but are not limited to antiwindup techniques, feedback linearization, sliding mode control, backstepping, flatness-based control, passivity- and dissipative-based methods, model predictive control, and potential- and Lagrangian-based methods. An additional challenge arises in the case of output feedback due to the fact that estimator-regulator separation does not hold in the nonlinear case.

Considering the diversity mentioned above, the mathematical rigor underlying these techniques ranges from heuristic techniques to rigorous methods, which typically rely on Lyapunov techniques. Among the proposed heuristic techniques is the state-dependent Riccati equation (SDRE) technique [1–4]. SDRE applies to nonlinear systems whose nonlinear dynamics $\dot{x} = f(x, u)$ can be cast in the *state-dependent coefficient* form $\dot{x} = A(x)x + B(x)u$. For these plants, the idea is to solve the algebraic Riccati equation for LQR at each time step as if the dynamics are instantaneously frozen in the form $A(x(t)), B(x(t))$. SDRE has been extensively tested in [5–11] in simulation, which provides confidence in the usefulness of this technique despite a dearth of theory.

A feature of SDRE is that the SDC parameterization is not unique, and thus the choice of SDC may impact stability and performance. At the same time, the SDC must be chosen so that $A(x(t)), B(x(t))$ is stabilizable at each point along the trajectory. This issue can be circumvented by replacing the algebraic Riccati equation used in SDRE with a differential Riccati equation. In conventional optimal control, however, this equation is integrated backwards in time, and this approach is therefore not feasible in cases where the future state is unknown.

An ad hoc solution to the requirement for backwards-in-time integration of the differential Riccati equation is proposed in [12, 13], where the differential Riccati equation is integrated *forward*, as in the case of the differential estimator Riccati equation. Although this *forward-propagating Riccati equation* (FPRE) technique introduces yet another heuristic element into SDC-based nonlinear control, it is shown in [14] that, at least in the case of linear time-invariant systems, the FPRE is stabilizing. Numerical simulation with time-varying plants whose future dynamics are not known (as in the case of linear parameter varying systems) as well as nonlinear systems [15, 16] suggests that FPRE provides a reliable and easily implementable, albeit heuristic, technique for a class of nonlinear systems.

The contribution of this study is the experimental evaluation of FPRE on a laboratory testbed and investigation of its performance. Experimental tests are performed on the Quanser 3 DOF Hover (3DH) testbed [17], which is a MIMO system with four actuators and six outputs. The dynamics of 3DH are nonlinear due to the coupling between the axes. Since the nonlinearities can be captured by an SDC model, this testbed is a candidate for FPRE control. To the best of our knowledge, this study is the first experimental evaluation of FPRE control. Furthermore, we compare the performance of FPRE with the performance of a conventional LQR controller for the reference commands near the linearization region, and away from the linearization region.

[1]Anna Prach and Erdal Kayacan are with the School of Mechanical and Aerospace Engineering, Nanyang Technological University, 639798, Singapore. annaprach@ntu.edu.sg, erdal@ntu.edu.sg

[2]Dennis S. Bernstein is with the Department of Aerospace Engineering, The University of Michigan, Ann Arbor, MI 48109-2140. dsbaero@umich.edu

This paper is organized as follows. Section II provides the formulation of FPRE control and SDC parameterization. Section III considers modeling of the testbed system, derivation of SDC model, and linearization. Experimental results for FPRE and LQR are covered in Section IV. Finally conclusions drawn from this study are given in Section V.

II. FPRE Control of Nonlinear Systems with SDC Models

Consider the nonlinear system

$$\dot{x}(t) = f(x(t), u(t)),\ x(0) = x_0, \tag{1}$$

where $x(t) \in \mathbb{R}^n$, $u(t) \in \mathbb{R}^m$, and, for all $x(t) \in \mathbb{R}^n$ and $u(t) \in \mathbb{R}^m$, $f(x(t), u(t)) \in \mathbb{R}^n$. We assume that (1) can be written in the SDC form [4]

$$\dot{x}(t) = A(x(t))x(t) + B(x(t))u(t), \tag{2}$$

where $A(x(t)) \in \mathbb{R}^{n\times n}$ and $B(x(t)) \in \mathbb{R}^{n\times m}$. A parameterization (2) exists under the assumptions $f \in \mathbb{C}^1$ and $f(0) = 0$. In addition, if $n \geqslant 2$, then $A(x(t))$ is not unique [3].

For full-state feedback, the FPRE control law is given by

$$u(t) = K(t)x(t), \tag{3}$$

where the feedback gain $K(t)$ is given by

$$K(t) = -R_2^{-1}B^{\mathrm{T}}(x(t))P(t)x(t), \tag{4}$$

and $P(t)$ is the solution of the forward-in-time Riccati equation

$$\begin{aligned}\dot{P}(t) &= A^{\mathrm{T}}(x(t))P(t) + P(t)A(x(t)) \\ &\quad - P(t)B(x(t))R_2^{-1}B^{\mathrm{T}}(x(t))P(t) + R_1,\ P(0) \geq 0,\end{aligned} \tag{5}$$

where $R_1 \in \mathbb{R}^{n\times n}$ is positive semidefinite and $R_2 \in \mathbb{R}^{n\times m}$ is positive definite. The weighting matrices R_1 and R_2 can also be state-dependent, i.e. $R_1(x(t))$, $R_2(x(t))$, which introduces additional degrees of freedom in the controller synthesis.

III. 3DH Testbed

The 3DH testbed [17] shown in Fig. 1 consists of a planar round frame with four propellers. The frame is mounted on a joint that enables the body to rotate about three axes. The propellers are driven by four DC motors. The lift force generated by the propellers is used to control the pitch and roll angles. Yaw control is done using the total torque generated by the propellers. The aim is to control the pitch and roll of the 3DH while maintaining constant yaw.

Fig. 1. Quanser 3 DOF Hover.

A. Nonlinear Dynamics

The nonlinear equations of motion of 3DH are given by

$$\dot{\phi} = p + \sin\phi\tan\theta\, q + \cos\phi\tan\theta\, r, \tag{6}$$

$$\dot{\theta} = \cos\phi\, q - \sin\phi\, r, \tag{7}$$

$$\dot{\psi} = \frac{\cos\phi}{\cos\theta}r + \frac{\sin\phi}{\cos\theta}q, \tag{8}$$

$$\dot{p} = \frac{J_{yy} - J_{zz}}{J_{xx}}qr + \frac{1}{J_{xx}}\tau_r, \tag{9}$$

$$\dot{q} = \frac{J_{zz} - J_{xx}}{J_{yy}}pr + \frac{1}{J_{yy}} + \frac{1}{J_{yy}}\tau_p, \tag{10}$$

$$\dot{r} = \frac{J_{xx} - J_{yy}}{J_{zz}}pq + \frac{1}{J_{zz}}\tau_y, \tag{11}$$

where ϕ, θ, ψ are the Euler angles, p, q, r are the angular rates in the body axes, J_{xx}, J_{yy}, J_{zz} are the moments of inertia, and τ_r, τ_p, τ_y are the torques acting on the roll, pitch, and yaw axes, respectively. Let V_{f}, V_{b}, V_{r}, V_{l} be the corresponding voltages of the front, back, right, and left motors. The torques are given by

$$\tau_r = LK_{\mathrm{f}}(V_{\mathrm{r}} - V_{\mathrm{l}}), \tag{12}$$

$$\tau_p = LK_{\mathrm{f}}(V_{\mathrm{f}} - V_{\mathrm{b}}), \tag{13}$$

$$\tau_y = K_{\mathrm{t}}(V_{\mathrm{r}} + V_{\mathrm{l}}) - K_{\mathrm{t}}(V_{\mathrm{f}} + V_{\mathrm{b}}), \tag{14}$$

where K_{f} is the thrust-force constant, K_{t} is the thrust-torque constant, and L is the distance between each propeller motor and the pivot on the axis. The parameters of 3DH are given in Table 1 [17].

Table 1. 3 DOF Hover Specification

Parameter	Value	Units
Pitch angle range	$\pm$37.5	deg
Yaw angle range	360	deg
Base dimension (L)	0.175	m
Moment of inertia around x-axis (J_{xx})	0.055	kg-m^2
Moment of inertia around y-axis (J_{yy})	0.055	kg-m^2
Moment of inertia around z-axis (J_{zz})	0.110	kg-m^2
Motor/propeller force-thrust constant (K_{f})	0.119	N/V
Motor/propeller torque thrust constant (K_{t})	0.0036	N-m/V

B. SDC Modelof 3DH

Define the state vector $x \triangleq [\phi, \theta, \psi, p, q, r]^{\mathrm{T}}$ and the control vector $u = [V_{\mathrm{f}}, V_{\mathrm{b}}, V_{\mathrm{r}}, V_{\mathrm{l}}]^{\mathrm{T}}$. From (6)–(11), an SDC dynamics matrix $A(x)$ and input matrix $B(x)$ for use with FPRE are given by

$$A(x) = \begin{bmatrix} 0 & 0 & 0 & 1 & \sin\phi\tan\theta & \cos\phi\tan\theta \\ 0 & 0 & 0 & 0 & \cos\phi & -\sin\phi \\ 0 & 0 & 0 & 0 & \frac{\sin\phi}{\cos\theta} & \frac{\cos\phi}{\cos\theta} \\ 0 & 0 & 0 & 0 & 0 & \frac{J_{yy}-J_{zz}}{J_{xx}}q \\ 0 & 0 & 0 & \frac{J_{zz}-J_{xx}}{J_{yy}}r & 0 & 0 \\ 0 & 0 & 0 & 0 & \frac{J_{xx}-J_{yy}}{J_{zz}}p & 0 \end{bmatrix}, \tag{15}$$

$$B(x) = \begin{bmatrix} 0 & 0 & 0 & 0 \\ 0 & 0 & 0 & 0 \\ 0 & 0 & 0 & 0 \\ 0 & 0 & \frac{LK_{\mathrm{f}}}{J_{xx}} & -\frac{LK_{\mathrm{f}}}{J_{xx}} \\ \frac{LK_{\mathrm{f}}}{J_{yy}} & -\frac{LK_{\mathrm{f}}}{J_{yy}} & 0 & 0 \\ -\frac{K_{\mathrm{t}}}{J_{zz}} & -\frac{K_{\mathrm{t}}}{J_{zz}} & \frac{K_{\mathrm{t}}}{J_{zz}} & \frac{K_{\mathrm{t}}}{J_{zz}} \end{bmatrix}. \tag{16}$$

C. Linearized Model

For use with LQR, a linearized model of 3DH at the hover condition $x = 0$ obtained using the Jacobian linearization is given by

$$\dot{x}(t) = Ax(t) + Bu(t), \tag{17}$$

where

$$A = \begin{bmatrix} 0 & 0 & 0 & 1 & 0 & 0 \\ 0 & 0 & 0 & 0 & 1 & 0 \\ 0 & 0 & 0 & 0 & 0 & 1 \\ 0 & 0 & 0 & 0 & 0 & 0 \\ 0 & 0 & 0 & 0 & 0 & 0 \\ 0 & 0 & 0 & 0 & 0 & 0 \end{bmatrix}, \tag{18}$$

and B is given by (16).

IV. LQR and FPRE Control of 3DH

To design an LQR controller we use the linearized dynamics A and B given by (18) and (16), whereas for FPRE we use the SDC matrices $A(x)$ and $B(x)$ given by (15) and (16). For both LQR and FPRE, we consider constant weighting matrices R_1 and R_2, where $R_1 = \mathrm{diag}(500, 400I_2, 20I_3)$ and $R_2 = 0.01I_4$. These choices of the weighting matrices are based on numerical testing. For FPRE, we choose $P(0) = I_6$.

For LQR the full-state feedback control law is given by

$$u(t) = Kx(t), \tag{19}$$

where the constant feedback gain is given by

$$K = -R_2^{-1}B^{\mathrm{T}}\bar{P}x(t), \tag{20}$$

and where $\bar{P}$ is the stabilizing solution of the algebraic Riccati equation

$$A^{\mathrm{T}}\bar{P} + \bar{P}A - \bar{P}BR_2^{-1}B^{\mathrm{T}}\bar{P} + R_1 = 0. \tag{21}$$

For the given A and B, the LQR feedback gain (20) is

$$K = \begin{bmatrix} -112 & 141 & 0 & -47 & 37 & 0 \\ -112 & -141 & 0 & -47 & -37 & 0 \\ 112 & 0 & 141 & 47 & 0 & 37 \\ 112 & 0 & -141 & 47 & 0 & -37 \end{bmatrix}. \tag{22}$$

A. Performance Evaluation of LQR and FPRE Control

In this subsection we compare the performance of LQR and FPRE for controlling the attitude of 3DH.

1) Step Commands: Consider step commands with height 5 deg at $t = 5$ sec for the pitch and roll angles, and zero commands for the yaw angle and the angular rates. Figures 2, 3, and 4 show the resulting Euler angles, angular rates, and input voltages, respectively. The feedback gains for the FPRE controller are given in Fig. 5. Results show that LQR and FPRE have similar resulting Euler angles and angular rates, and also require similar control effort.

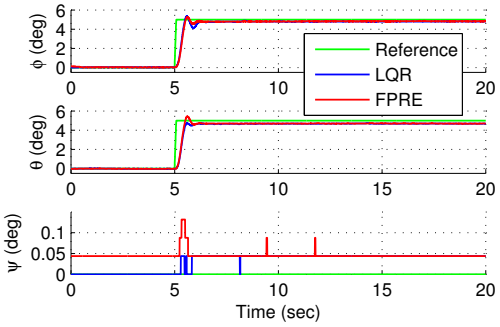

Fig. 2. Euler angles for pitch and roll step commands with height 5 deg.

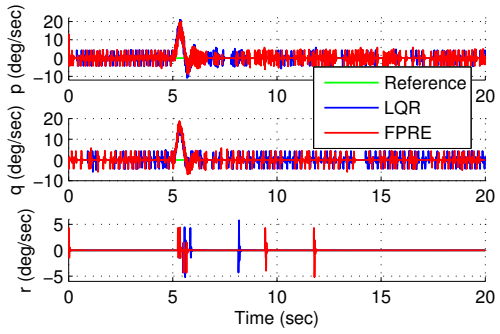

Fig. 3. Angular rate for pitch and roll step commands with height 5 deg.

Next, we increase the height of the step command for the pitch and roll angles to 15 deg, while using zero references for the yaw angle and angular rates. Figures 6, 7, and 8 show the resulting Euler angles, angular rates, and input voltages, respectively. The feedback gains for the FPRE controller are given in Fig. 9. In this case, FPRE provides faster convergence than LQR and less oscillation for the Euler angles and angular rates. Also, FPRE requires less control effort than LQR, and thus less frequent input saturation occurs.

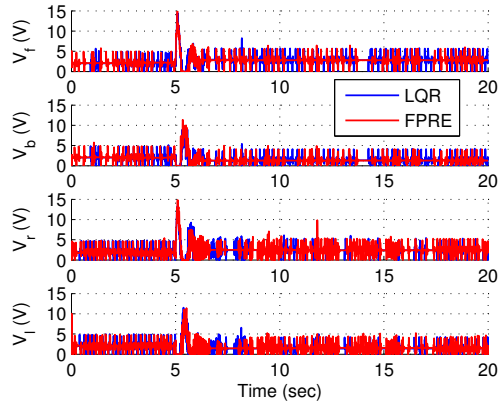

Fig. 4. Control input voltages for pitch and roll step commands with height 5 deg.

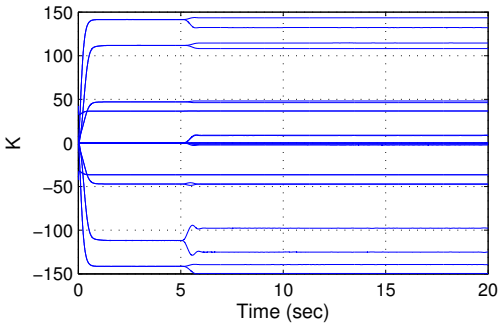

Fig. 5. Evolution of the FPRE feedback gains for pitch and roll step commands with height 5 deg.

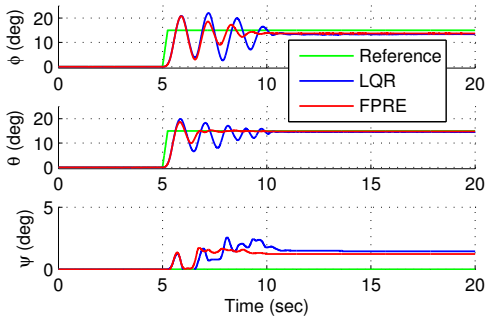

Fig. 6. Euler angles for pitch and roll step commands with height 15 deg.

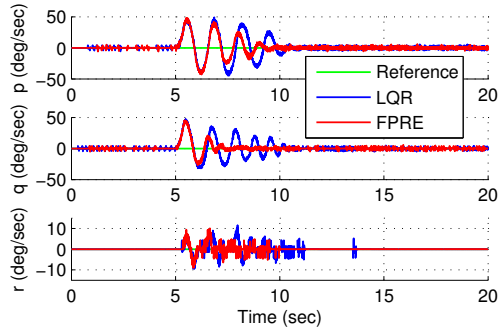

Fig. 7. Angular rate for pitch and roll step commands with height 15 deg.

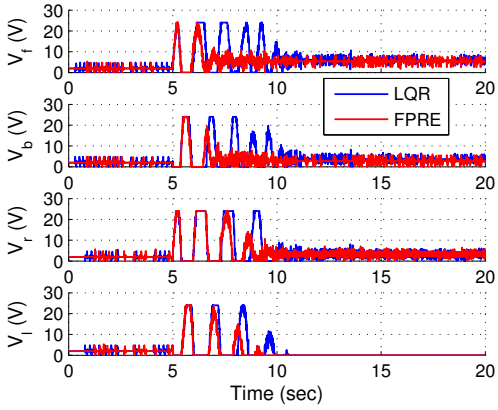

Fig. 8. Control input voltages for pitch and roll step commands with height 15 deg.

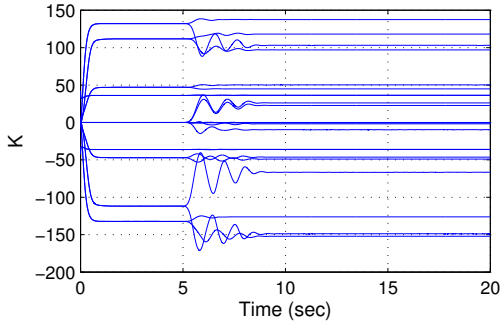

Fig. 9. Evolution of the FPRE feedback gains for pitch and roll step commands with height 15 deg.

2) Harmonic Commands: Consider harmonic commands with amplitude 15 deg and frequency 1 rad/sec for the pitch and roll angles, and zero commands for the yaw angle and angular rates. The resulting Euler angles, angular rates, and input voltages are given in Fig. 10, 11, and 12, respectively. The feedback gains for the FPRE controller are given in Fig. 13. In this case, LQR and FPRE have similar resulting Euler angles, however, FPRE exhibits more oscillations than LQR in the roll rate response. Figure 12 shows that LQR requires less control effort than FPRE.

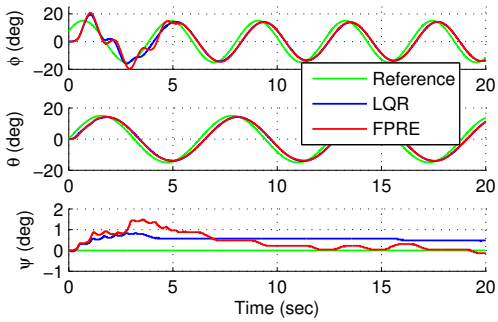

Fig. 10. Euler angles for pitch and roll harmonic commands with amplitude 15 deg and frequency 1 rad/sec.

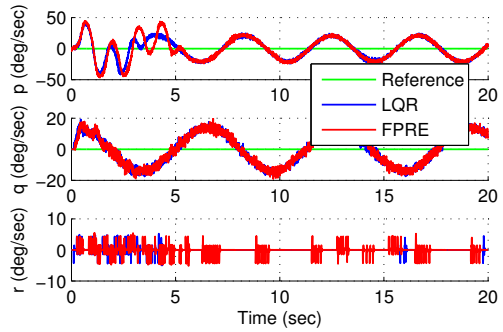

Fig. 11. Angular rates for pitch and roll harmonic commands with amplitude 15 deg and frequency 1 rad/sec.

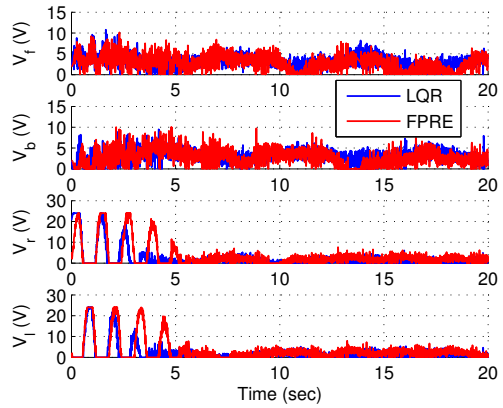

Fig. 12. Control input voltages for pitch and roll harmonic commands with amplitude 15 deg and frequency 1 rad/sec.

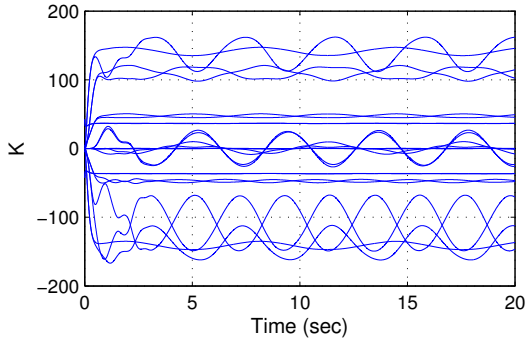

Fig. 13. Evolution of the FPRE feedback gains for pitch and roll harmonic commands with amplitude 15 deg and frequency 1 rad/s.

Next, we increase the amplitudes of the harmonic commands for the pitch and roll angles to 30 deg, while keeping zero commands for the yaw angle and angular rates. Figures 14, 15, and 16 show the resulting Euler angles, angular rate, and input voltages, respectively. The feedback gains for the FPRE controller are given in Fig. 17. In this case, LQR fails to provide an accurate command following for the roll angle, however, LQR and FPRE show similar performance for the pitch and yaw command following. Figure 15 shows that FPRE has a more oscillatory transient response, and FPRE and LQR have similar response for the pitch and yaw angular rates. However, LQR exhibits poor performance in the roll rate response. As can be seen from Fig. 16, both FPRE and LQR include saturation in the transient responses. For LQR, saturation in the right and left motors occur due to poor performance in the roll channel.

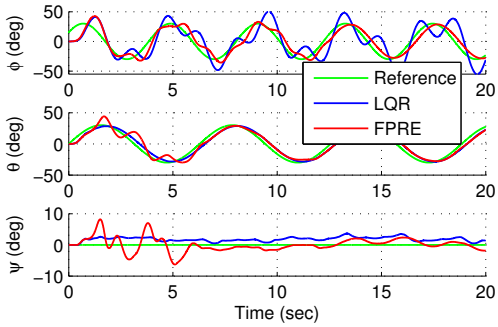

Fig. 14. Euler angles for pitch and roll harmonic commands with amplitude 30 deg and frequency 1 rad/sec.

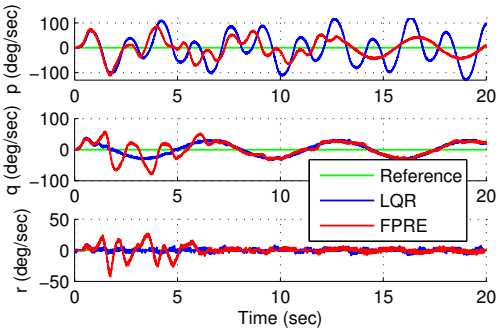

Fig. 15. Angular rate for pitch and roll harmonic commands with amplitude 30 deg and frequency 1 rad/sec.

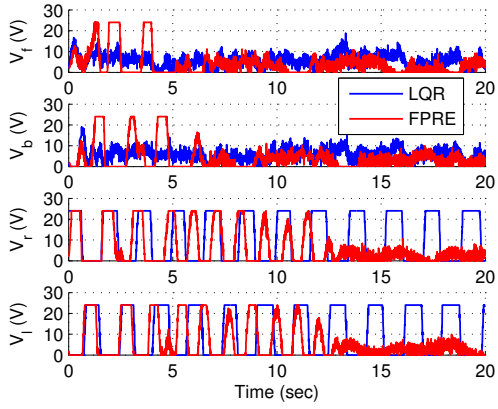

Fig. 16. Control input voltages for pitch and roll harmonic commands with amplitude 30 deg and frequency 1 rad/sec.

B. Analysis and Discussion

In these experiments we studied two cases corresponding to commands near the linearization region, and away from the linearization region due to commands with large amplitudes. The weighing matrices R_1 and R_2 are constant for all

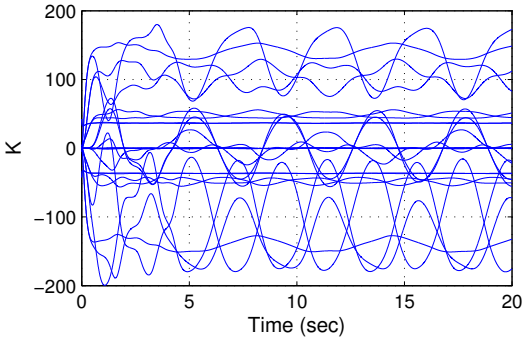

Fig. 17. Evolution of the FPRE feedback gains for pitch and roll harmonic commands with amplitude 30 deg and frequency 1 rad/s.

test cases and chosen such that both FPRE and LQR provide similar reference command following for the references near the equilibrium used for linearization.

The results show that for small commands, the FPRE and LQR responses are very similar, which is expected. However, the command-following performance of FPRE is significantly better than the performance of LQR for large commands. In this case the system is driven away from the equilibrium used for LQR design, and as a result we observe degradation in the LQR performance. The ability of FPRE to account for the nonlinear plant dynamics yields superior performance relative to LQR

V. Conclusions

In this study, the performance of FPRE control is investigated through real-time experiments on the Quanser 3 DOF Hover testbed. The LQR and FPRE responses are compared for the angular position reference command following problem. The experimental tests carried out in this study show the potential of FPRE for nonlinear control problems due to the update algorithm of the feedback gains in real-time throughout the operating envelope that was tested. Future research will focus on applying FPRE to a quadrotor with six-degree-of-freedom motion and aerodynamic effects. Suggestions for future work include investigation of the effect of the choice of state-dependent weighting matrices on the performance of FPRE.

References

[1] C. P. Mracek and J. R. Cloutier, "Control Designs for the Nonlinear Benchmark Problem via the State-Dependent Riccati Equation Method," *Int. J. Robust Nonlinear. Contr.*, vol. 8, pp. 401–433, 1998.

[2] J. R. Cloutier and D. T. Stansbery, "The Capabilities and Art of State-Dependent Riccati Equation-Based Design," in *Proc. Amer. Contr. Conf.*, Anchorage, AK, May 2002, pp. 86–91.

[3] T. Cimen, "Systematic and Effective Design of Nonlinear Feedback Controllers via the State-Dependent Riccati Equation (SDRE) method," *Annual Reviews of Control*, vol. 34, pp. 32–51, 2010.

[4] ——, "Survey of State-Dependent Riccati Equation in Nonlinear Optimal Feedback Control Synthesis," *J. Guid. Control Dynam.*, vol. 35, pp. 1025–1047, 2012.

[5] J. R. Cloutier and P. H. Zipfel, "Hypersonic Guidance via the State-Dependent Riccati Equation Control Method," in *Proc. IEEE Int. Conf. Contr. Appl.*, Kohala Coast, HI, August 1999, pp. 219–224.

[6] D. K. Parrish and D. R. Ridgely, "Attitude Control of a Satellite Using the SDRE Method," in *Proc. Amer. Contr. Conf.*, Albuquerque, NM, June 1997, pp. 942–946.

[7] A. Bogdanov and E. Wan, "State-Dependent Riccati Equation Control for Small Autonomous Helicopters," *J. Guid. Control Dynam.*, vol. 30, pp. 47–60, 2007.

[8] N. Bhoir and S. N. Singh, "Control of Unsteady Aeroelastic System via State-Dependent Riccati Equation Method," *J. Guid. Control Dynam.*, vol. 28, pp. 78–84, 2005.

[9] E. B. Erdem and A. Alleyne, "Design of a Class of Nonlinear Controllers via State Dependent Riccati Equations," *IEEE Trans. Contr. Syst. Tech.*, vol. 12, pp. 2986–2991, 2004.

[10] T. Yucelen, A. S. Sadahalli, and F. Pourboghrat, "Online Solution of State Dependent Riccati Equation for Nonlinear System Stabilization," in *Proc. Amer. Contr. Conf.*, Baltimore, MD, June 30 – July 2 2010, pp. 6336–6341.

[11] A. Ratnoo and D. Ghose, "State-Dependent Riccati-Equation-Based Guidance Law for Impact-Angle-Constrained Trajectories," *J. Guid. Control Dynam.*, vol. 32, pp. 320–326, 2009.

[12] M. S. Chen and C. Y. Kao, "Control of Linear Time-Varying Systems Using Forward Riccati Equation," *J. Dyn. Syst., Meas. Contr.*, vol. 119, no. 3, pp. 536–540, 1997.

[13] A. Weiss, I. Kolmanovsky, and D. S. Bernstein, "Forward-Integration Riccati-Based Output-Feedback Control of Linear Time-Varying Systems," in *Proc. Amer. Contr. Conf.*, Montreal, Canada, June 2012, pp. 6708–6714.

[14] A. Prach, O. Tekinalp, and D. S. Bernstein, "Infinite-Horizon Linear-Quadratic Control by Forward Propagation of the Differential Riccati Equation," *IEEE Contr. Sys. Mag.*, vol. 35, April 2015.

[15] ——, "A Numerical Comparison of Frozen-Time and Forward-Propagating Riccati Equations for Stabilization of Periodically Time-Varying Systems," in *Proc. Amer. Contr. Conf.*, Portland, OR, June 2014, pp. 5633–5638.

[16] ——, "Faux-Riccati Synthesis of Nonlinear Observer-Based Compensators for Discrete-Time Nonlinear Systems," in *Proc. Conf. Dec. Contr.*, Los Angeles, CA, December 2014, pp. 854–859.

[17] "Quanser – 3 DOF Hover," http://www.quanser.com/products.